Matrix Infrared Spectra of Dihydrido Cyclic and Trihydrido Ethynyl Products from Reactions of Th and U Atoms with Ethylene Molecules

Han-Gook Cho[†] **and Lester Andrews***[,‡]

Department of Chemistry, University of Incheon, 177 Dohwa-dong, Nam-ku, Incheon, 402-749, South Korea, and Department of Chemistry, University of Virginia, P.O. Box 400319, Charlottesville, Virginia 22904-4319

Received: January 20, 2009; Revised Manuscript Received: February 25, 2009

Reactions of laser-ablated thorium and uranium atoms with ethylene isotopomers have been carried out and the primary products identified in the matrix IR spectra. The dihydrido cyclic and trihydrido ethynyl products ($MH_2-C_2H_2$ and MH_3CCH) are identified from the matrix spectra of both Th and U, whereas the insertion product absorption is observed only in the U spectra. The present results indicate that C−H insertion and following H migration from C to M also occur in reaction of the actinides with ethylene. Formation of the trihydrido ethynyl products is parallel to the previous results of group 4 metals. Metal hydride (MH_x) absorptions are not observed in the infrared spectra, suggesting that the H_2 elimination from the dihydrido cyclic intermediate is relatively slow. Density functional theory calculations reproduce the vibrational characteristics of the identified products and the relative stabilities. The cyclic triangular $ThH_2-C_2H_2$ system with two π electrons is aromatic, which contributes to the unique stability of this thorium dihydrido cyclic product.

Introduction

The hydrocarbon C−H bonds, once considered chemically inactive, are now becoming a common subject for insertion reactions, providing chances to prepare precursors for more valuable end products.[1−3] The following rearrangements expand the possibilities to generate related transient species, which allow insights to understand the key steps for numerous synthetic reactions and catalytic processes.[4] Recent studies have shown that transition metals are effective C−H bond insertion agents and often proceed to form simple, distinct complexes showing unique structures and intriguing photochemical properties.[2,3] These small metal complexes also serve as model systems to investigate the properties and reactivity of large transition metal complexes because they are more amenable to high level of theoretical approaches.

Elimination of H_2 in reaction of ethylene with early transition metal atoms (particularly the early second row transition metals) has been examined in previous reaction dynamics studies, and the details about the reaction path have been the subject of theoretical studies as well.[5−8] The results reveal that group 4 metals are the most reactive. It is also generally accepted that H_2 elimination by transition metal atoms proceeds in the order of M + ethylene → π-complex → metallacyclopropane → insertion product → dihydrido cyclic complex → M-C_2H_2 + H_2.[9] The first formed weak π complex converts into the more strongly bound complex (metallacyclopropane). It then undergoes C−H insertion to form MH-$CHCH_2$ and later rearranges to a dihydrido cyclic product ($MH_2-C_2H_2$). Finally, H_2 elimination is believed to occur from the dihydrido product, leaving a metal−acetylene complex.

Recently the insertion and dihydrido cyclic complexes were identified in the matrix IR spectra from reactions of groups 4−6 metals atoms with ethylene isotopomers, providing strong evidence for the suggested reaction path for the H_2 elimination.[10−13] It is also interesting that the unexpected trihydrido ethynyl complex (MH_3-CCH) is identified from reactions of group 4 metals, indicating that a second H migration occurs from C to M.[11] Binary metal hydride (MH_x) absorptions are also observed in the groups 4 and 5 metal spectra, which provides evidence for H_2 elimination.[11,12] Density functional theory (DFT) calculations show that H_2 elimination from the group 6 metal dihydrido cyclic complex is energetically less favorable, consistent with absence of the metal hydride absorptions.[13]

Interestingly enough, the actinides are also effective C−H bond insertion agents. The insertion and other primary products formed via H migration such as the first actinide methylidene $CH_2{=}ThH_2$ have been observed in previous studies.[14] In this study we report matrix IR spectra from reactions of laser-ablated Th and U atoms with ethylene isotopomers. The primary products via C−H insertion and following rearrangements are identified, parallel to the early transition metals. While they are similar to those from reactions of group 4 metals, no metal hydride absorptions are observed, suggesting that the H_2-elimination process is considerably slow. DFT computations reproduce the stability of the products and their vibrational characteristics.

Experimental and Computational Methods

The experimental apparatus has been described previously.[3,15] Laser-ablated Th and U atoms, produced by laser ablation of metal targets (Oak Ridge National Laboratory) with a Nd:YAG laser (5 to 20 mJ/pulse), were reacted with C_2H_4, C_2D_4, $^{13}C_2H_4$ (Cambridge Isotope Laboratories, 99%), and CH_2CD_2 (MSD Isotopes) in excess argon during condensation at 10 K using a closed-cycle refrigerator (Air Products Displex). Reagent gas mixtures ranged 0.5−1.0% in argon. After reaction, infrared spectra were recorded at a resolution of 0.5 cm^{-1} using a Nicolet 550 spectrometer with an MCT-B detector. Samples were later irradiated for 20 min periods by a mercury arc street lamp (175 W) with the globe removed and a combination of optical filters and subsequently annealed to allow further reagent diffusion.[15]

* To whom correspondence should be addressed. E-mail: lsa@virginia.edu.
[†] University of Incheon.
[‡] University of Virginia.

10.1021/jp900610c CCC: $40.75
Published on Web 03/31/2009

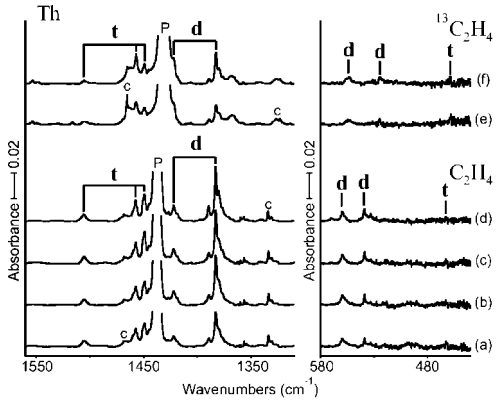

Figure 1. IR spectra in the regions of 1560−1310 and 580−440 cm^{-1} for laser-ablated Th atoms codeposited with C_2H_4 and $^{13}C_2H_4$ in excess argon at 10 K and their variation. (a) Th + 0.5% C_2H_4 in Ar codeposited for 1 h. (b) The same as part a after photolysis with $\lambda > 420$ nm. (c) The same as part b after photolysis with $240 < \lambda < 380$ nm. (d) The same as part c with annealing to 28 K. (e) Th + 0.5% $^{13}C_2H_4$ in Ar codeposited for 1 h. (f) The same as part e after photolysis with $240 < \lambda < 380$ nm. d and t denote the product absorption groups. P and c designate the precursor and common absorptions.

To support the assignment of new experimental frequencies and to correlate with our previous investigations,[11−13] similar DFT calculations were carried out using the Gaussian 03 package,[16] B3LYP density functional,[17] 6-311++G(3df,3pd) basis sets for C, H,[18] and the small (60 electron) core SDD pseudopotential and basis set[19] for Th and U to provide a consistent set of vibrational frequencies for the reaction products. Geometries were fully relaxed during optimization, and the optimized geometry was confirmed by vibrational analysis. BPW91[20] calculations were also done to complement the B3LYP results. The vibrational frequencies were calculated analytically, and the zero-point energy is included in the calculation of binding energies. Previous investigations have shown that DFT calculated harmonic frequencies are usually slightly higher than observed frequencies,[3,11−15,21] depending on the mode anharmonicity, and they provide useful predictions for infrared spectra of new molecules.

Results and Discussion

Reactions of laser-ablated thorium and uranium atoms with ethylene isotopomers were carried out, and the matrix infrared spectra of new products will be compared with frequencies calculated by density functional theory.

Th + C_2H_4. Figure 1 shows the C_2H_4 and $^{13}C_2H_4$ spectra in the Th−H stretching and low frequency regions. Two sets of product absorptions marked **"d"** and **"t"** (**d** and **t** for di- and trihydrido products) are observed on the basis of the intensity variations upon photolysis and annealing. The **d** absorptions increase about 40 and 10% on visible ($\lambda > 420$ nm) and UV ($240 < \lambda < 380$ nm) irradiation, respectively, and gradually decrease in the process of annealing, whereas the **t** absorptions remain almost the same on visible photolysis but increase about 30% on UV irradiation. The observed frequencies of the **d** and **t** absorptions are listed in Table 1 and compared with the DFT computed frequencies in Tables 2 and 3.

The **d** absorptions in the Th−H stretching region at 1422.2 and 1383.1 cm^{-1} with about 1:3 intensity ratio have their D counterparts at 1013.1 and 989.3 cm^{-1} (H/D ratios of 1.403 and 1.398) as shown in Figure 2 and show negligible ^{13}C shifts as listed in Tables 1 and 2. These are similar to bands at 1435.7 and 1397.1 cm^{-1} observed for the Th−H stretching modes of the methylidene $CH_2{=}ThH_2$ complex.[14b] They are also compared with the hydrogen stretching frequencies of 1480.1 and 1455.6 cm^{-1} for ThH_2, 1435.4 and 1434.1 cm^{-1} for ThH_3, and 1444.8 and 1443.3 cm^{-1} for ThH_4 and the deuterium counterparts of 1055.6 and 1040.3 cm^{-1} for ThD_2, 1025.9 and 1024.8 cm^{-1} for ThD_3, and 1032.1 and 1031.1 cm^{-1} for ThD_4.[22] Binary thorium hydride absorptions are not observed in this study. The metal hydride absorptions are observed in the previous matrix studies of groups 4 and 5 metals with ethylene but not in the group 6 metal studies. The results are correlated with the energies of the hydrogen elimination products relative to the dihydrido cyclic products ($MH_2-C_2H_2$).[11−13]

The two strong Th−H stretching d absorptions indicate that a primary reaction product with a ThH_2 moiety is generated in reaction of Th with ethylene. It is most probably a dihydrido complex ($ThH_2-C_2H_2$) on the basis of the previous studies,[5,6,9−13] and these bands are due to the symmetric and antisymmetric ThH_2 stretching modes, as the slightly lower H/D ratio and stronger absorption are appropriate for the antisymmetric motion. The ThH_2 symmetric stretching mode is evidently mixed with the C=C stretching mode, whose frequency is expected about 30 cm^{-1} higher than the ThH_2 stretching band. However, the C=C stretching absorption is most probably covered by the precursor CH_2 scissoring band. The **d** absorption at 559.9 cm^{-1} has its D and ^{13}C counterparts at 508.2 and 554.1 cm^{-1} (H/D and 12/13 ratios of 1.102 and 1.010) and is assigned to the ThC_2 symmetric stretching mode of the cyclic product on the basis of the frequency, isotopic shifts, and agreements with DFT values. Another low frequency **d** absorption at 539.0 cm^{-1} has its D and ^{13}C counterparts at 468.1 and 516.3 cm^{-1} (H/D and 12/13 ratios of 1.151 and 1.044) and is assigned to the ThC_2 antisymmetric stretching mode. Both the symmetric and antisymmetric stretching modes are highly mixed with the ThH_2 scissoring mode.

The CH_2CD_2 spectra shown in Figure 3 provide further structural information for the dihydrido product. The **d** Th−H and Th−D stretching absorptions are observed at the centers (1402.8 and 1001.7 cm^{-1}) of the symmetric and antisymmetric ThH_2 and ThD_2 stretching frequencies, strong evidence that the two Th−H bonds are the same. The low frequency **d** absorptions at 523.1 and 478.4 cm^{-1} also correlate with the predicted ThC_2 symmetric and antisymmetric stretching bands for the half-deuterated dihydrido product. The good agreement between the four observed frequencies for each isotopomer and the predicted values (Table 2) substantiate formation of the dihydrido cyclic complex ($ThH_2-C_2H_2$) with two equal Th−H bonds in reaction of the actinide metal atoms and ethylene. The Th dihydrido cyclic complex is in line with those of the early transition metals prepared and studied earlier.[5,6,9−13]

The **t** absorptions observed at 1505.5, 1457.4, and 1449.3 cm^{-1} in Figure 1 show essentially no ^{13}C shift but have the D counterparts at 1037.1 and 1036.1 cm^{-1} (H/D ratios of 1.405 and 1.399) in Figure 2. The high-frequency Th−D stretching absorption is believed covered. These three Th−H stretching absorptions strongly suggest that another major product with probably three Th−H bonds is also generated in the Th reaction, which is similar to the group 4 metal trihydrido ethynyl complex.[11] The **t** Th−H stretching absorptions are also observed in the CH_2D_2 spectra (Figure 3). The low frequency **t** absorption at 463.0 cm^{-1} has its ^{13}C counterpart at 459.3 cm^{-1}, but the D counterpart is believed to be beyond our observation range. It is assigned to the ThH_3 deformation mode of the ThH_3-CCH in the singlet ground state as shown in Table 3.

TABLE 1: Frequencies of Product Absorptions Observed from Reactions of Th with Ethylene in Excess Argon[a]

	C_2H_4	C_2D_4	$^{13}C_2H_4$	CH_2CD_2	description
t	1950.0, 1949.2	1838.1, 1837.6	1879.8, 1879.1	1949.0, 1838.0	A_1 C≡C str.
	1505.5		1505.4		A_1 ThH_3 str.
	1457.4, 1450.4, 1449.3	1037.1, 1036.1	1456.8, 1450.2, 1449.3	1456.6, 1059.0, 1049.4, 1037.0	E ThH_3 str.
	463.0		459.3		A_1 ThH_3 deform
d	1422.2	1013.1	1421.7	1402.8	A′ ThH_2 s. str.
	1383.1	989.3	1382.9	1001.7	A″ ThH_2 as. str.
	559.9	508.2	554.1	523.1	A′ ThC_2 s. str.
	539.0	468.1	516.3	478.4	A′ ThC_2 as. str.

[a] All frequencies are in cm^{-1}. Description gives major coordinate. **d** and **t** stand for dihydrido and trihydrido products, respectively.

TABLE 2: Observed and Calculated Frequencies of the Fundamental Bands of $ThH_2-C_2H_2$ in its Ground $^1A'$ State[a]

	$ThH_2-C_2H_2$				$ThD_2-C_2D_2$				$ThH_2-^{13}C_2H_2$				ThHD−CHCD			
description	obs[b]	BPW91[c]	B3LYP[d]	int[d]	obs[b]	BPW91[c]	B3LYP[d]	int[d]	obs[b]	BPW91[c]	B3LYP[d]	int[d]	obs[b]	BPW91[c]	B3LYP[d]	int[d]
A′ C−H str.		3064.2	3127.6	19		2279.4	2326.7	3		3053.4	3116.6	20		3028.0	3093.8	28
A′ C−H str.		3022.2	3088.0	27		2223.1	2271.1	9		3013.0	3078.6	28		2264.1	2311.0	5
A′ C═C str.		1417.7	1437.3	90		1351.2	1388.6	9		1415.5	1374.4	41		1401.1	1413.4	186
A′ ThH_2 s. str.	1422.2	1388.4	1415.2	283	1013.1	1002.4	1008.2	182	1421.7	1338.9	1424.9	333	1402.8	1368.9	1398.4	387
A″ ThH_2 as. str.	1383.1	1384.9	1384.5	803	989.3	983.3	983.0	411	1382.9	1384.9	1384.5	802	1001.7	992.7	995.5	324
A′ HCCH IP as. bend	.	1091.7	1135.5	82		916.6	949.2	35		1074.9	1118.5	83		1034.5	1074.4	55
A″ HCCH OOP as. bend		967.9	999.5	0		765.5	790.2	0		958.6	990.0	0		891.7	919.5	3
A′ HCCH IP s. bend		808.6	843.8	16		581.5	606.6	0		807.8	843.0	18		674.1	700.5	7
A″ HCCH OOP s. bend		632.3	646.4	54		482.3	492.6	32		628.4	642.5	53		535.9	545.9	58
A′ ThC_2 s. str.	559.9	553.2	556.0	220	508.2	505.5	506.1	121	554.1	544.7	548.0	219	523.1	523.0	526.9	158
A′ ThC_2 as. str.	539.0	522.9	520.0	91	468.1	449.0	449.9	65	516.3	510.7	506.9	84	478.4	476.7	476.2	71
A′ ThH_2 scis.		478.8	474.0	13		358.7	358.2	36		470.2	464.9	14		438.0	438.7	25
A″ ThH_2 twist		385.9	378.5	6		275.0	270.9	3		385.7	378.2	6		352.7	331.0	43
A′ ThH_2 wag		328.2	292.1	164		238.2	211.0	87		326.8	291.3	161		258.2	242.7	85
A″ ThH_2 lock		256.2	241.8	58		197.5	189.6	25		253.9	239.0	60		216.8	203.2	41

[a] Frequencies and intensities are in cm^{-1} and km/mol. [b] Observed in an argon matrix. [c] Frequencies computed with BPW91/6-311++G(3df,3pd). [d] Frequencies and intensities computed with B3LYP/6-311++G(3df, 3pd). SDD core potential and basis set are used for Th. $ThH_2-C_2H_4$ has a C_s structure.

TABLE 3: Observed and Calculated Frequencies of the Fundamental Bands of ThH_3-CCH in its Ground $^1A'$ State[a]

	ThH_3-CCH				ThD_3-CCD				$ThH_3-^{13}C^{13}CH$			
description	obs[b]	BPW91[c]	B3LYP[d]	int[d]	obs[b]	BPW91[c]	B3LYP[d]	int[d]	obs[b]	BPW91[c]	B3LYP[d]	int[d]
A_1 CH s. str.		3367.3	3435.5	30		2592.7	2651.3	1		3350.2	3417.9	32
A_1 C≡C str.	1950.0	1968.2	2036.4	95	1838.1	1847.4	1906.9	112	1879.8	1897.3	1963.1	86
A_1 ThH_3 str.	1505.5	1465.6	1494.7	380		1037.5	1058.1	189	1505.4	1465.5	1494.7	380
E ThH_3 str.	1457.4, 1449.3	1410.4	1431.5	800 × 2	1036.1	1000.9	1015.9	407 × 2	1456.8, 1449.3	1410.4	1431.5	800 × 2
E HCC bend		691.9	728.9	35 × 2		548.1	578.0	14 × 2		685.2	721.8	36 × 2
E ThH_3 deform		551.3	549.5	59 × 2		391.8	390.5	26 × 2		551.1	549.3	62 × 2
A_1 ThH_3 deform	463.0	478.1	486.8	380		372.4	377.3	242	459.3	477.3	486.0	374
A_1 Th−C str.		352.0	351.1	30		315.0	315.8	14		340.6	339.7	31
E ThH_3 rock		324.1	328.6	113 × 2		249.0	250.6	70 × 2		322.0	326.7	107 × 2
E CCTh bend		104.0	111.7	2 × 2		90.5	97.7	1 × 2		101.2	108.5	2 × 2

[a] Frequencies and intensities are in cm^{-1} and km/mol. [b] Observed in an argon matrix. [c] Frequencies computed with BPW91/6-311++G(3df,3pd). [d] Frequencies and intensities computed with B3LYP/6-311++G(3df, 3pd). SDD core potential and basis set are used for Th. ThH_3-CCH has a C_{3v} structure with three equivalent Th−H bonds.

Moreover, Figure 4 shows the C≡C stretching product absorptions. The heavy Th atom is a good isolator for the C≡C stretching motion, and therefore, its frequency would clearly show the effects of D and ^{13}C substitution for the H−C≡C moiety, regardless of the isotopic composition of the ThH_3 moiety. The **t** absorption pair at 1950.0 and 1949.2 cm^{-1}, which are most probably split by the matrix and ∼10 and ∼20 cm^{-1} lower than the corresponding values in the Zr and Hf cases,[11] have their D counterparts at 1838.1 and 1837.6 cm^{-1} (H/D ratios of both 1.061) and ^{13}C counterparts at 1879.8 and 1879.1 cm^{-1} (12/13 ratios of both 1.037). Moreover, the **t** absorptions at 1949.0 and 1838.0 cm^{-1} in the CH_2CD_2 spectra show minimal isotopic shifts from the values of the corresponding isotopomers. The good correlation of the observed frequencies with the predicted values for the five vibrational modes of the Th trihydrido ethynyl complex including the C≡C stretching mode as shown in Table 3 support formation of ThH_3-CCH.

DFT computations also show that the dihydrido cyclic and trihydrido ethynyl complexes are the most stable among the plausible products. $ThH_2-C_2H_2$ and ThH_3-CCH in the singlet ground states are 64.2 and 59.7 kcal/mol more stable than the reactants ($Th(^3F) + C_2H_4$), whereas the insertion product ($ThH-CHCH_2$), metallacyclopropane ($Th-C_2H_4$), and dihydrido vinylidene complex ($ThH_2=C=CH_2$) in their singlet ground states are only 43.4, 37.8, and 44.0 kcal/mol more stable than reactants, respectively. On the other hand, in the triplet states the dihydrido cyclic and trihydrido ethynyl complexes are much higher in energy than the insertion complex as shown

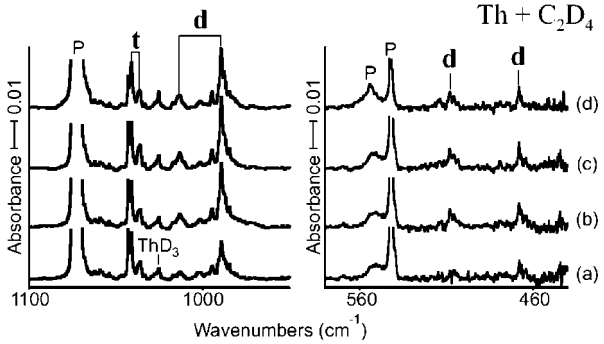

Figure 2. IR spectra in the regions of 1100−950 and 580−440 cm^{-1} for laser-ablated Th atoms codeposited with C_2D_4 in excess argon at 10 K and their variation. (a) Th + 0.5% C_2D_4 in Ar codeposited for 1 h. (b) As in part a after broadband photolysis with $\lambda > 420$ nm. (c) As in part b after photolysis with $240 < \lambda < 380$ nm. (d) As in part c after annealing to 28 K. d and t denote the product absorption groups. P designates the precursor absorption.

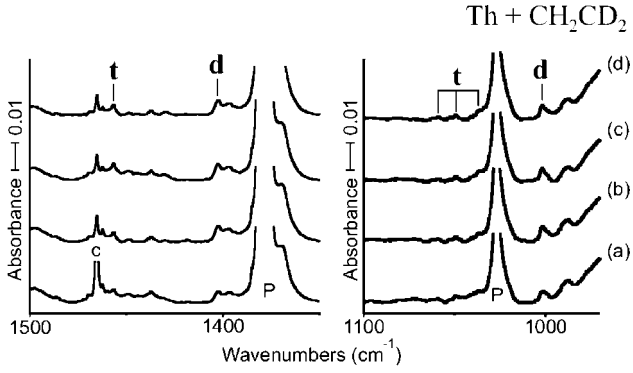

Figure 3. IR spectra in the regions of 1500−1350 and 1100−970 cm^{-1} for laser-ablated Th atoms codeposited with CH_2CD_2 in excess argon at 10 K and their variation. (a) Th + 1.0% CH_2CD_2 in Ar codeposited for 1 h. (b) As in part a after broadband photolysis with $\lambda > 420$ nm. (c) As in part b after photolysis with $240 < \lambda < 380$ nm. (d) As in part c after annealing to 28 K. i and d denote the product absorption groups. d and t denote the product absorption groups. P and c designate the precursor and common absorptions.

in Figure 5. The present results suggest that the reaction probably proceeds in the singlet potential surface. If it occurs on the triplet surface, the insertion complex and metallacyclopropane would be the primary products.

In contrast to the dihydrido cyclic and trihydrido ethynyl complexes, the insertion complex is not identified in the Th matrix IR spectra, similar to the case of the group 5 metals. The insertion complex is 20.8 kcal/mol higher than the dihydrido cyclic complex, which is comparable with the energy differences for the group 5 metals.[6f,12] The transition state between the insertion and dihydrido complexes in the singlet states is 13.2 kcal/mol higher than the insertion complex. The DFT frequencies of the unobserved insertion complex are listed in Table S1 of Supporting Information. The metallacyclopropane absorptions, on the other hand, are predicted to be mostly very weak (Table S2 of Supporting Information), in line with the previous cases.[11−13] The stronger ones are the C−C stretching band (30 km/mol infrared intensity) and ThC_2 symmetric and antisymmetric stretching bands (29 km/mol), and the absence of these product absorptions indicates that the metal complex is not formed and isolated in the matrix in a measurable amount. The energetically less favorable vinylidene products have not been observed in the previous studies with early transition-metals,[5,6,9−13] and such a product is not identified in this study either. Its strong ThH_2 scissoring band, which would appear at ∼500 cm^{-1}, is not observed, while the ThH_2 stretching frequencies are predicted to be similar to those of the dihydrido cyclic product.

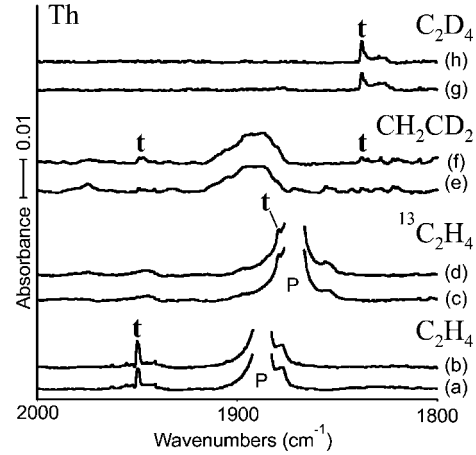

Figure 4. IR spectra in the region of 2000−1800 cm^{-1} for laser-ablated Th atoms codeposited with C_2H_4 isotopomers in excess argon at 10 K and their variation. (a) Th + 0.5% C_2H_4 in Ar codeposited for 1 h. (b) As in part a after broadband photolysis with $240 < \lambda < 380$ nm. (c) Th + 0.5% $^{13}C_2H_4$ in Ar codeposited for 1 h. (d) As in part c after broadband photolysis with $240 < \lambda < 380$ nm. (e) Th + 1.0% CH_2CD_2 in Ar codeposited for 1 h. (f) As in part e after broadband photolysis with $240 < \lambda < 380$ nm. (g) Th + 0.5% C_2D_4 in Ar codeposited for 1 h. (h) As in part g after broadband photolysis with $240 < \lambda < 380$ nm. t denotes the trihydrido product absorption, and P stands for the precursor band.

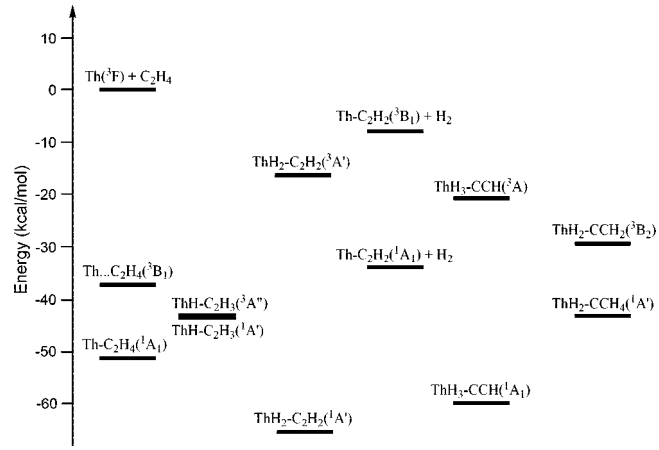

Figure 5. The energies of the plausible products relative to the reactants (Th(^{3}F) + ethylene). Notice that the dihydrido cyclic and trihydro ethynyl complexes in the singlet ground states are the most stable ones. The C−H insertion and following rearrangement probably occur in the singlet potential surface on the basis of the fact that the di and trihydrido complexes are identified, but the insertion complex is not.

Figure 6 illustrates the B3LYP structures of the plausible products from reactions of Th atoms with ethylene. The metallacyclopropane, insertion, dihydrido cyclic, dihydrido vinylidene, and trihydrido ethynyl complexes have C_{2v}, planar C_s, C_s, C_s, and C_{3v} structures, respectively. Parallel to the previous studies for groups 4 and 5 metals,[11,12] the C−M and C−C bond lengths decrease in the order of metallacyclopropane, insertion, and dihydrido complexes. The longer C−C bond of the metallacyclopropane complex reflects the fact that it is essentially a single bond. The natural bond orbital (NBO) analysis[16,23] describes a single bond with 28.6% s and 71.0% p characters. Because of the high strain in the cyclic structure, the C−Th bonds in the metallacyclopropane have low s

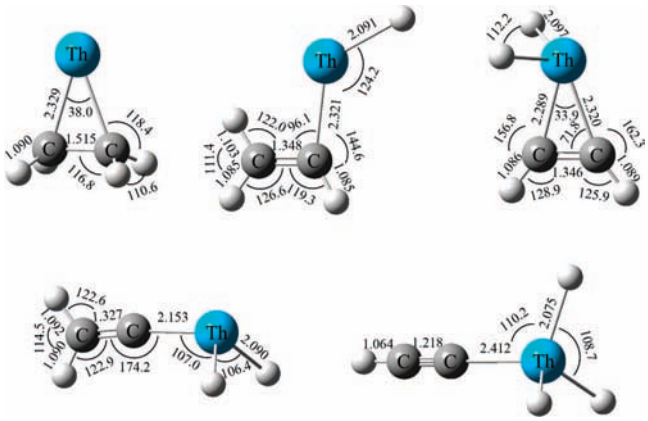

Figure 6. The B3LYP structures of the plausible products from reaction of Th atoms with ethylene. The dihydrido cyclic and trihydrido ethynyl complexes are identified from the matrix IR spectra, which are also the most stable complexes among the plausible ones as shown in Figure 5. The π complex has a C_{2v} structure; the insertion, dihydrido cyclic, and vinylidene complexes have a C_s structure, and the trihydrido ethynyl product has a C_{3v} structure. The illustrated structures are in the singlet ground states except for the insertion complex in the triplet state.

character (13.4%) from the carbon atom, which is compared with the relatively high s character (22.2%) in the insertion complex.

The dihydrido cyclic complex has shorter C−C and C-M bonds. While the metal atom in a higher oxidation state tends to form a stronger bond,[24] stronger back donation to the C−C π^* orbital is also expected in the dihydrido complex than in the insertion product, further strengthening the C−M bonds. Interestingly enough, the NBO occupancies of the C−Th σ^* orbitals for the dihydrido complex (0.044 and 0.019) are higher than those of the C−C π^* obital (0.014), suggesting that the back donation in fact occurs to the cyclic π system rather than just to the C−C π^* obital. The cyclic triangular system with two π electrons can be considered as a small metal containing aromatic system, which contributes to the unique stability of the dihydrido cyclic product.[5,6,9−13]

NBO analyses also reveal that the C−Th bond of the vinylidene complex, which is much shorter than those of the metallacyclicpropane, insertion, and dihydrido cyclic complexes, is a double bond. Its C−C bond length (1.327 Å) is compared with that of ethylene (1.325 Å) computed at the same level of theory. The C−C bond length of the trihydrido complex (1.218 Å) is compared with the computed value for acetylene (1.196 Å).

U + C_2H_4. Shown in Figure 7 are the product matrix IR spectra in the U−H stretching absorption region from reactions of U with ethene isotopomers. The product absorptions are generally weaker than those in the Th spectra described above as U appears to be less reactive than Th under these conditions. Three sets of product absorptions marked **d**, **t**, and **i** are observed on the basis of the intensity variations on photolysis and annealing. The **d** absorptions double on visible irradiation but decrease to the original intensity on UV irradiation, whereas the **t** absorptions stay almost the same on visible photolysis but double on UV irradiation. The weaker **i** absorptions decrease on visible irradiation but increase to twice the original intensity on UV irradiation. The product absorption frequencies are listed in Table 4 and compared with DFT values in Tables 5−7.

The **d** absorption at 1411.3 cm^{-1} shows no ^{13}C shift and its D counterpart at 1009.6 cm^{-1} (H/D ratio of 1.398) as illustrated in Figure 8. In the C_2D_4 spectra, another **d** absorption is observed at 1024.7 cm^{-1}; however, the H counterparts in the C_2H_4 and

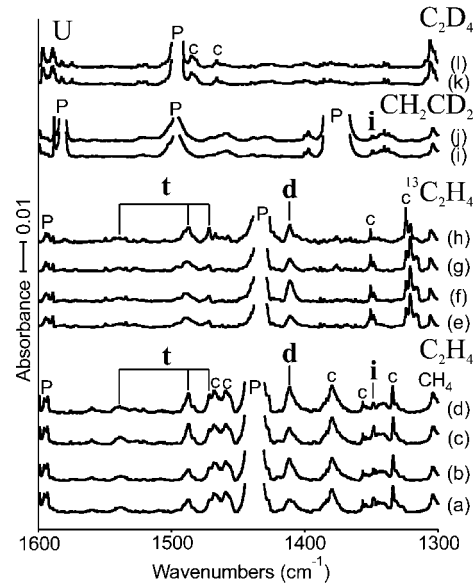

Figure 7. IR spectra in the regions of 1600−1300 cm^{-1} for laser-ablated U atoms codeposited with C_2H_4 and $^{13}C_2H_4$ in excess argon at 10 K and their variation. (a) U + 0.5% C_2H_4 in Ar codeposited for 1 h. (b) As in part a after photolysis with $\lambda > 420$ nm. (c) As in part b after photolysis with $240 < \lambda < 380$ nm. (d) As in part c with annealing to 28 K. (e) U + 0.5% $^{13}C_2H_4$ in Ar codeposited for 1 h. (f) As in part e after photolysis with $\lambda > 420$ nm. (g) As in part f after photolysis with $240 < \lambda < 380$ nm. (h) As in part g annealing to 28 K. d, i, and t denote the product absorption groups. P, c, and CH_4 designate the precursor, common, and residual CH_4 absorptions, which is formed by cracking of the pump oil vapor.

TABLE 4: Frequencies of Product Absorptions Observed from Reactions of U with Ethylene in Excess Argon[a]

	C_2H_4	C_2D_4	$^{13}C_2H_4$	CH_2CD_2	description
t	1947.0	1826.1	1876.2	1946.8, 1835.8	A_1 C≡C str.
	1539.1	1091.8	1539.1	[b]	A′ UH_3 s. str.
	1487.4	1066.0	1487.4	[b]	A′ UH_3 as. str.
	1472.0	1053.8	1472.0	[b]	A″ UH_3 as. str.
d		1009.6		1425.5	A′ UH_2 s. str.
	1411.3	1024.7	1411.3	1041.3	A″ UH_2 as. str.
	1092.8	867.2	1073.2		A′ HCCH IP as. bend
	543.3	506.9	529.6		A′ UC_2 s. str.
i	1348.4, 1344.8	952.4	[b]	1349.4	U−H str.

[a] All frequencies are in cm^{-1}. Description gives major coordinate. **t**, **d**, and **i** stand for trihydrido, dihydrido, and insertion products, respectively. [b] Covered by precursor absorption.

$^{13}C_2H_4$ spectra, expected near 1432 cm^{-1}, are unfortunately covered by a precursor absorption. The observed H and D stretching frequencies are compared with the U−H stretching frequencies of 1461.1 and 1425.4 cm^{-1} for the $CH_2{=}UH_2$ complex,[25] of 1399.0 and 1365.3 cm^{-1} for UH_2, 1346.8 cm^{-1} for UH_3, and 1483.6 and 1481.7 cm^{-1} for UH_4 and U−D stretching frequencies of 1044 and 1016 cm^{-1} for the $CD_2{=}UD_2$ complex, of 998.3 and 975.7 cm^{-1} for UD_2, 962.5 cm^{-1} for UD_3, and 1060.7 and 1059.8 cm^{-1} for UD_4.[25] None of the UH_x absorptions are observed in this study. A trace of the very strongly absorbing NUN molecule is observed at 1051.0 cm^{-1}.[26]

Following the Th and other previous cases[11] and computation results, the **d** U−H and U−D stretching absorptions are assigned to the U dihydrido cyclic complex (UH_2−C_2H_2). The U−H stretching band of the insertion complex is expected below 1360 cm^{-1}, slightly lower than the frequencies of UH_2,[3,25] and the

TABLE 5: Observed and Calculated Frequencies of the Fundamental Bands of $UH_2-C_2H_2$ in its Ground $^3A'$ State[a]

	$UH_2-C_2H_2$				$UD_2-C_2D_2$				$UH_2-{}^{13}C_2H_2$				UHD−CHCD			
description	obs[b]	BPW91[c]	int[c]	B3LYP[d]	int[d]	obs[b]	BPW91[c]	int[c]	B3LYP[d]	int[d]	obs[b]	BPW91[c]	int[c]	B3LYP[d]	int[d]	obs[b]	BPW91[c]	int[c]	B3LYP[d]	int[d]
A′ C_2-H_2 s. str.		3073.8	11	3144.0	11		2292.3	1	2343.4	1		3062.6	12	3132.7	12		3045.0	18	3106.5	20
A′ C_2-H_2 as. str.		3037.6	18	3101.0	20		2232.6	7	2280.6	7		3028.5	19	3091.6	21		2271.7	4	2325.8	4
A′ UH_2 s. str.		1463.1	402	1487.3	266	1009.6	1033.7	239	1045.6	214		1461.2	437	1481.2	365	1425.5	1406.9	435	1482.6	417
A″ UH_2 as. str.	1411.3	1392.4	244	1485.4	489	1024.7	990.6	325	1057.2	242	1411.3	1396.8	630	1485.2	490		1030.6	285	1061.2	144
A′ C═C str.		1404.8	476	1439.8	169		1355.4	15	1402.3	15		1350.8	53	1392.5	68		1375.1	117	1421.5	62
A′ HCCH IP as. bend	1092.8	1038.1	72	1105.3	79	867.2	877.6	31	929.7	34	1073.2	1021.4	74	1088.0	81	1003.0	978.8	70	1042.9	120
A″ HCCH OOP as. bend		909.2	0	987.4	98		722.6	0	762.8	0		900.0	1	982.5	111		842.4	7	907.7	41
A″ UH_2 twist		286.5	48	857.2	207		205.9	25	661.6	142		286.1	47	848.2	195	[c]	214.2	12	766.4	220
A′ HCCH IP s. bend		748.7	9	807.8	18		535.7	1	584.4	0		747.9	9	806.7	20		627.7	7	672.8	7
A″ HCCH OOP s. bend		605.8	64	631.6	131		460.6	44	469.4	87		602.5	63	628.9	127		504.8	42	519.1	111
A′ UC_2 s. str.	543.3	451.2	55	548.2	199	506.9	440.2	46	506.7	118	529.6	439.3	62	536.0	202		456.7	88	528.4	143
A′ UC_2 as. str.		492.9	49	505.3	97		420.2	61	436.0	55		480.7	45	493.7	98		453.1	72	462.8	62
A′ UH_2 scis.		510.7	123	459.8	35		354.2	26	337.1	42		508.8	117	454.5	27		407.5	39	411.1	47
A′ UH_2 wag		101.4	119	303.9	142		90.9	71	220.3	80		96.9	115	302.6	138		94.9	127	254.7	98
A″ UH_2 lock		161.8	80	246.1	38		127.5	31	185.4	15		160.6	82	244.5	39		143.8	55	207.0	24

[a] Frequencies and intensities are in cm^{-1} and km/mol. [b] Observed in an argon matrix. [c] Frequencies and intensities computed with BPW91/6-311++G(3df,3pd). [d] Frequencies and intensities computed with B3LYP/6-311++G(3df, 3pd). SDD core potential and basis set are used for U. $UH_2-C_2H_2$ has a C_s structure with B3LYP but a C_1 structure with BPW91. Mode descriptions and symmetries are for C_s structure.

trihydrido complex absorptions are normally weaker than those for the dihydrido complex. The latter applies to the original deposition spectrum before subsequent photolysis because formation of the trihydrido complex requires another H migration.[11]

As shown in Figure 8, the **d** absorption at 1092.8 cm^{-1} has its D and ^{13}C counterparts at 867.2 and 1073.2 cm^{-1} (H/D and 12/13 ratios of 1.260 and 1.018). On the basis of the frequency and the sizeable D and small ^{13}C shifts, it is assigned to HCCH in-plane bending mode. Another **d** absorption in the low-frequency region at 543.3 has its D and ^{13}C counterparts at 506.9 and 529.6 cm^{-1} (H/D and 12/13 ratios of 1.072 and 1.026), and it is assigned to the UC_2 symmetric stretching mode on the basis of the frequency and sizable ^{13}C shift. Table 5 shows that the observed **d** absorptions are in fact the strong bands predicted for the dihydrido cyclic complex, supporting formation of the uranium dihydrido cyclic complex in reaction with ethylene.

It is also noticeable in Table 5 that the symmetric UH_2 and the C═C stretching modes are strongly coupled particularly in B3LYP frequency calculation, which result in switching the order of the symmetric and antisymmetric UH_2 stretching frequencies, which are just a few inverse centimeters apart. However, such a frequency reversal does not occur in the BPW91 frequencies, due to the larger difference of the two frequencies. The two DFT methods yield two different structures for the dihydrido cyclic complex as well. A C_s structure with the two equivalent U−H bonds is predicted by B3LYP and a C_1 structure with two different U−H bonds by BPW91, leading to the larger difference in the UH_2 stretching frequencies.

The **t** U−H stretching absorptions at 1539.1, 1487.4, and 1472.0 cm^{-1} have their D counterparts at 1091.8, 1066.0, and 1053.8 (H/D ratios of 1.410, 1.395, and 1.397), respectively, and show no ^{13}C shifts. These three U−H stretching absorptions indicate that parallel to the Th and group 4 metal cases, the U trihydrido complex (UH_3-CCH) is produced in reaction with ethylene. Figure 9 provides more evidence, the C≡C stretching absorptions and relevant isotopic shifts of the trihydrido complex. While they are weaker than Th counterparts, the observed stretching frequencies are 2.3−3.6 cm^{-1} lower than the corresponding values for the Th trihydrido isotopomers described above (the B3LYP frequencies are 3.1−4.2 cm^{-1} lower). The C≡C stretching absorption at 1947.0 cm^{-1} has D and ^{13}C counterparts at 1835.8 and 1876.2 cm^{-1} (H/D and 12/13 ratios of 1.061 and 1.038). The absorptions at 1946.8 and 1835.8 cm^{-1} in the CH_2CD_2 spectra show negligible shifts from the values of corresponding isotopomers. As shown in Table 6, the observed t absorptions are in fact the strong bands predicted for the U trihydrido ethynyl complex (UH_3-CCH) in the triplet ground state. However, the UH_3 deformation band, which is also predicted to be strong, is unfortunately too close to our observation limit to observe.

A weak **i** U−H stretching absorption is observed at 1348.4 cm^{-1}, and its D counterpart is at 952.3 cm^{-1} (H/D ratio of 1.416), while the ^{13}C counterpart is covered by a common absorption in the $^{13}C_2H_4$ spectra. On the basis of the relatively low frequency, the product absorption is probably due to the U insertion complex, $UH-CHCH_2$, while no other i absorptions are observed due to their very low absorption intensities (Table 7). Unlike the case of Th, where the insertion complex is far less stable than the dihydrido cyclic and trihydrido ethynyl products, the U insertion product is the most stable product as shown in Figure 10. They are predicted to be 28.5, 26.6, and 13.0 kcal/mol more stable than the reactants ($U(^5L) + C_2H_4$), respectively, and the higher oxidation-state complexes are

TABLE 6: Observed and Calculated Frequencies of the Fundamental Bands of UH_3-CCH in its Ground $^3A'$ State[a]

	UH_3-CCH				UD_3-CCD				UH_3-$^{13}C^{13}CH$			
description	obs[b]	BPW91[c]	B3LYP[d]	int[d]	obs[b]	BPW91[c]	B3LYP[d]	int[d]	obs[b]	BPW91[c]	B3LYP[d]	int[d]
A′ C−H str.		3369.9	3435.9	33		2590.5	2650.2	2		3353.0	3418.3	35
A′ C═C str.	1947.0	1951.7	2032.0	89	1835.8	1834.6	1903.7	107	1876.2	1881.2	1958.8	80
A′ UH_3 s. str.	1539.1	1527.8	1568.7	411	1091.8	1081.5	1110.6	206	1539.1	1527.8	1568.6	412
A′ UH_3 as. str.	1487.4	1475.6	1500.7	827	1066.0	1047.0	1065.0	421	1487.4	1475.6	1500.7	827
A″ UH_3 as. str.	1472.0	1478.4	1492.7	738	1053.8	1049.0	1059.0	376	1472.0	1478.4	1492.7	738
A′ CCH bend		663.9	773.1	33		525.7	582.0	13		657.6	725.9	34
A″ CCH bend		688.0	713.5	39		545.8	565.4	15		681.3	706.6	40
A′ UH_3 scis.		564.3	579.2	41		404.0	411.6	22		563.7	579.1	41
A″ UH_3 scis.		504.6	523.5	89		358.6	371.1	47		504.5	523.5	89
A′ UH_3 deform		459.3	475.4	344		363.9	377.3	203		458.4	474.1	336
A′ C−U str.		345.6	350.1	19		304.7	307.4	18		334.5	339.1	22
A″ UH_3 rock		302.7	338.5	78		234.5	260.9	47		300.5	336.2	76
A′ UH_3 rock		280.1	308.7	113		218.8	239.8	71		277.8	306.4	110
A″ CCU bend		105.3	116.2	1		90.9	101.0	0		102.5	113.0	1
A′ CCU bend		100.4	109.4	0		85.5	94.1	0		97.9	106.5	0

[a] Frequencies and intensities are in cm^{-1} and km/mol. [b] Observed in an argon matrix. [c] Frequencies computed with BPW91/6-311++G-(3df,3pd). [d] Frequencies and intensities computed with B3LYP/6-311++G(3df, 3pd). SDD core potential and basis set are used for U. UH_3-CCH has a C_s structure with two equal U−H bonds with both B3LYP and BPW91.

TABLE 7: Calculated Frequencies of the Fundamental Bands of UH-$CHCH_2$ in its Ground ^5A State[a]

	UH−$CHCH_2$				UD−$CDCD_2$				UH−$^{13}CH^{13}CH_2$			
description	obs[b]	BPW91[c]	B3LYP[d]	int[d]	obs[b]	BPW91[c]	B3LYP[d]	int[d]	obs[b]	BPW91[c]	B3LYP[d]	int[d]
C−H str.		3077.9	3121.7	24		2283.0	2315.9	9		3067.6	3111.1	24
C−H str.		3047.2	3094.9	22		2242.4	2278.8	10		3038.1	3085.7	22
C−H str.		2783.3	2926.3	36		2036.0	2140.6	18		2776.4	2919.0	37
C═C str.		1552.2	1608.3	1		1422.8	1501.9	2		1528.0	1576.5	2
CH_2 scis.		1363.0	1424.4	17		1042.0	1075.6	11		1335.8	1395.6	18
U−H str.	1348.4	1326.1	1338.6	549	952.4	940.6	948.8	274	[e]	1320.8	1338.5	547
HCCH IP s. bend		1166.4	1233.6	9		960.5	1007.3	6		1149.9	1217.0	10
HCCH OOP bend		950.8	1039.8	1		728.3	792.7	10		946.2	1036.0	2
CH_2 wag	[c]	857.1	961.1	55	[c]	663.5	744.6	24		849.1	950.7	54
HCCH IP as. bend		847.1	915.1	15		616.1	665.8	7		844.4	912.5	14
C−U str.		442.4	460.3	74		395.3	415.3	54		430.3	447.7	72
CH_2 twist		317.2	355.1	22		241.2	266.4	13		315.2	353.1	22
CUH bend		216.7	305.1	63		188.1	219.5	32		212.7	304.5	62
UH OOP bend		187.7	189.7	83		138.9	129.2	38		185.8	190.4	84
CCU bend		70.3	172.0	16		49.2	154.5	13		70.3	167.3	14

[a] Frequencies and intensities are in cm^{-1} and km/mol. [b] Observed in an argon matrix. [c] Frequencies computed with BPW91/6-311++G-(3df,3pd). [d] Frequencies and intensities computed with B3LYP/6-311++G(3df, 3pd). SDD core potential and basis set are used for U. UH−$CHCH_2$ has a C_1 structure. [e] Covered.

believed to be stabilized more in the matrix, because of interaction of the more polarized bonds with the matrix host.[3,11−13] As with Th, we found no evidence for the U metallacyclopropane complex (frequencies given in Table S3 of Supporting Information).

Figure 10 shows the energies of the plausible products relative to the reactants computed without accounting for spin orbit coupling. For the methane system, the inclusion of spin orbit coupling lowered the energy of triplet relative to quintet products.[25] In general the products are less stable relative to the reactants in comparison with the Th case, consistent with the lower yields for the products. Unlike the case of Th, the U insertion complex is predicted to be the most stable product, which is analogous to the methane product systems.[14b,25] In view of the products identified (the insertion, dihydrido cyclic, and trihydrido complexes), the reaction probably begins on the quintet potential energy surface and crosses to the triplet surface. If the reaction proceeded on the quintet surface, the dihydrido cyclic complex would be a minor product, and if formed, H_2 elimination would likely follow. We found no evidence in the matrix infrared spectra for the U acetylene complex or uranium hydrides, which would be formed in the reaction of U and H_2 released from the dihydro complex.[14c,25a]

Figure 11 illustrates the plausible product structures (B3LYP) from reaction of U and ethylene. The metallacyclopropane, insertion, dihydrido cyclic, dihydrido vinylidene, and trihydrido ethynyl complexes have C_{2v}, C_1, C_s, C_1 (close to C_s), and C_s (close to C_{3v}) structures in their ground electronic states, respectively. In the insertion complex, the U, two C, and three H atoms form a near-planar structure, and the remaining H atom bonded to the metal atom is located slightly above it. The C−C bond length of the metallacyclopropane complex is again longer than those of the insertion and dihydrido cyclic complexes, indicating that it is essentially a single bond. The C−C bonds of the insertion and dihydrido cyclic complexes (both 1.336 Å) are, however, longer than that of the vinylidene complex (1.319 Å), due to back donation. The NBO occupation numbers of the C−U σ^* bonds for the dihydrido cyclic complex (0.0373 and 0.0462) are again larger than those of the C−C π^* bond (0.0220), showing again that the back donation occurs to the UC_2 triangular π system rather than just to the C−C π^* orbital.

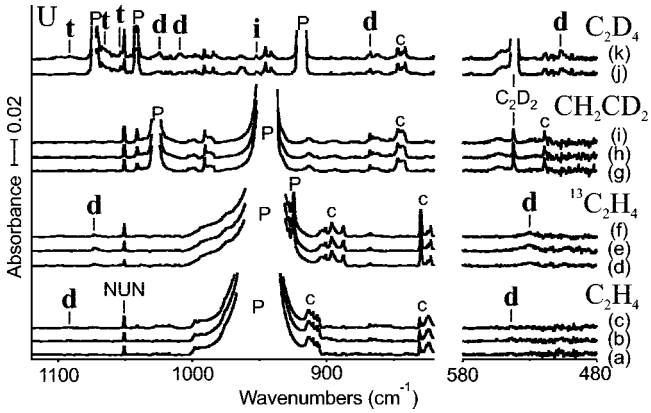

Figure 8. IR spectra in the regions of 1120−820 and 580−480 cm^{-1} for laser-ablated U atoms codeposited with ethylene isotopomers in excess argon at 10 K and their variation. (a) U + 0.5% C_2H_4 in Ar codeposited for 1 h. (b) As in part a after photolysis with $\lambda > 420$ nm. (c) As in part b after photolysis with $240 < \lambda < 380$ nm. (d) U + 0.5% $^{13}C_2H_4$ in Ar codeposited for 1 h. (e) As in part d after photolysis with $\lambda > 420$ nm. (f) As in part e after photolysis with $240 < \lambda < 380$ nm. (g) U + 1.0% CH_2CD_2 in Ar codeposited for 1 h. (h) As in part g after photolysis with $\lambda > 420$ nm. (i) After photolysis with $240 < \lambda < 380$ nm. (j) U + 0.5% C_2D_4 in Ar codeposited for 1 h. (k) After photolysis with $\lambda > 220$ nm. d, i, and t denote the product absorption groups. P, c, and C_2D_2 designate the precursor, common, and C_2D_2 absorption, which is produced by plume photolysis of C_2D_4.

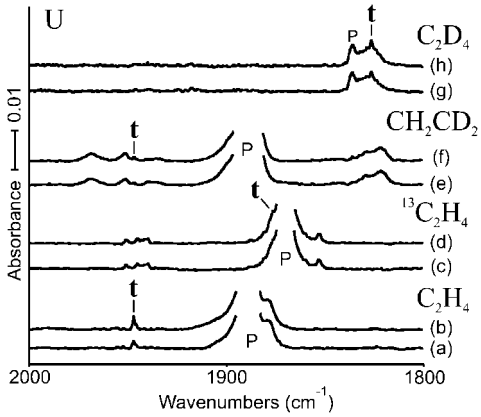

Figure 9. IR spectra in the regions of 2000−1800 cm^{-1} for laser-ablated U atoms codeposited with ethylene isotopomers in excess argon at 10 K and their variation. (a) U + 0.5% C_2H_4 in Ar codeposited for 1 h. (b) As in part a after photolysis with $240 < \lambda < 380$ nm. (c) U + 0.5% $^{13}C_2H_4$ in Ar codeposited for 1 h. (d) As in part c after photolysis with $240 < \lambda < 380$ nm. (e) U + 1.0% CH_2CD_2 in Ar codeposited for 1 h. (f) As in part e after photolysis with $240 < \lambda < 380$ nm. (g) U + 0.5% C_2D_4 in Ar codeposited for 1 h. (h) As in part g after photolysis with $\lambda > 220$ nm. t denotes the trihydrido product absorption, and P stands for the precursor band.

Unlike the B3LYP structure, the BPW91 dihydrido cyclic complex has a C_1 structure with two different U−H bonds as described above. The C−U bond of the vinylidene complex is a double bond (2.194 Å), which is much shorter than those of the other complexes (2.263−2.352 Å). The U trihydrido ethynyl complex has a C_s structure. It is very close to a C_{3v} structure, but with the C_{3v} constraint, it gives imaginary frequencies for the UH_3 deformation modes. The C−C bond length of 1.218 Å is essentially the same as that for the Th counterpart (ThH_3−CCH), consistent with the similar C−C stretching frequencies, and compared with that of 1.196 Å for acetylene at the same level of computation.

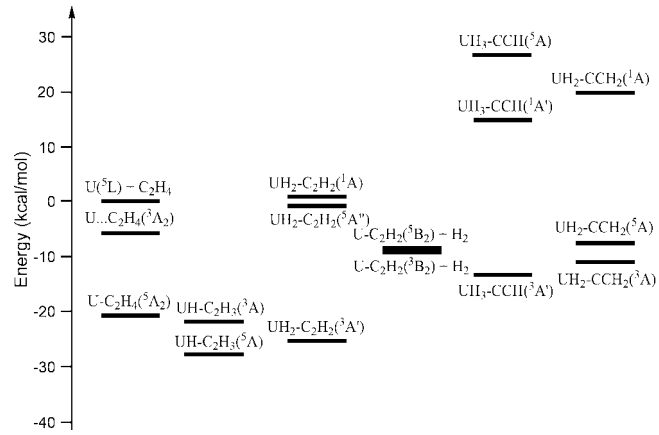

Figure 10. The energies of the plausible products relative to the reactants (U(^{5}L) +ethylene). Notice that UH−$CHCH_2$(Q) is the most stable, while UH_2−C_2H_2(T) and UH_3−CCH(T) are almost as stable. The three complexes are identified form the matrix IR spectra.

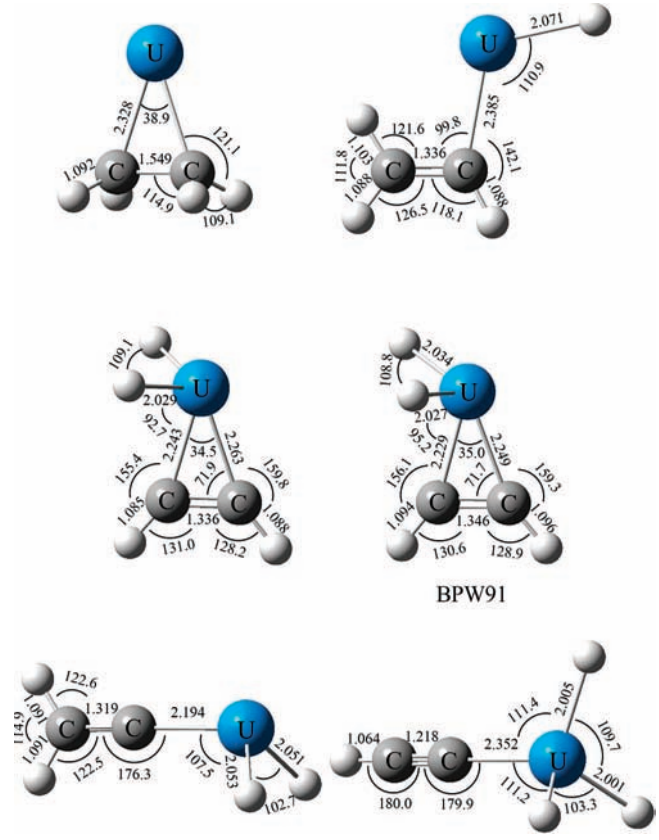

Figure 11. The B3LYP structures of the plausible products from reaction of U atoms with ethylene in their ground electronic states. The insertion, dihydrido cyclic, and trihydrido ethynyl complexes are identified from the matrix IR spectra, which are also the most stable complexes among the plausible ones as shown in Figure 10. The metallacyclopropane complex has a C_{2v} structure, and the insertion, dihydrido cyclic, vinylidene, and trihydrido ethynyl complexes have a C_s structure. The dihydrido cyclic complex has a C_1 structure with two different U−H bonds with BPW91 and the trihydrido complex structure is close to a C_{3v} structure.

Conclusions

Reactions of laser-ablated Th and U atoms with ethylene have been carried out, and the primary products are identified in the matrix IR spectra on the basis of their vibrational characteristics. The dihydrido cyclic and trihydrido ethynyl complexes are identified from reactions of Th with ethylene isotopomers while

the absorptions from the insertion along with the di and trihydrido complexes are observed in the U spectra. The present results reveal that C−H insertion and following H migration also take place in reactions of the actinides with ethylene to form the dihydrido cyclic complexes. While the dihydrido product is considered as the key reaction intermediate for H_2 elimination,[9] no metal hydride absorptions are observed, suggesting that unlike the cases of the groups 4 and 5 metals[11,12] the H_2 elimination from the actinide dihydrido cyclic complex is slow. Absence of the insertion complex in the Th spectra is traced to the substantially higher energy of the product. The second H migration from the C to metal atom leads to formation of the Th and U trihydrido ethynyl complexes, supporting the general perception that the actinides are chemically similar to the group 4 metals. The DFT calculations reproduce the observed vibrational characteristics of the identified products and their relative stabilities in comparison to other possible reaction products.

Acknowledgment. We gratefully acknowledge financial support from the National Science Foundation (U.S.) Grant CHE 03-52487 to L.A. and support from the Korea Institute of Science and Technology Information (KISTI) by Grant No. KSC-2008-S02-0001.

Supporting Information Available: Tables of calculated frequencies for related unobserved species. This material is available free of charge via the Internet at http://pubs.acs.org.

References and Notes

(1) (a) Davies, H. M.; Beckwith, R. E. J. *Chem. Rev.* **2003**, *103*, 2861. (b) Hall, C.; Perutz, R. N. *Chem. Rev.* **1996**, *96*, 3125. (c) Campos, K. R. *Chem. Soc. Rev.* **2007**, *36*, 1069.

(2) (a) Proctor, D. L.; Davis, H. F. *Proc. Natl. Acad. Sci.* **2008**, *105*, 12677. (b) Davis, S. C.; Klabunde, K. J. *J. Am. Chem. Soc.* **1978**, *100*, 5973. (c) Billups, W. E.; Konarski, M. M.; Hauge, R. H.; Margrave, J. L. *J. Am. Chem. Soc.* **1980**, *102*, 7393.

(3) Andrews, L.; Cho, H.-G. *Organometallics* **2006**, *25*, 4040. and references therein (Review article).

(4) (a) Olson, D. E.; Du Bois, J. *J. Am. Chem. Soc.* **2008**, *130*, 11248. (b) Shilov, A. E.; Shul'pin, G. B. *Chem. Rev.* **1997**, *97*, 2879.

(5) (a) Yi, S. S.; Blomberg, M. R. A.; Siegbahn, P. E. M.; Weisshaar, J. C. *J. Phys. Chem. A* **1998**, 102. (b) Reichert, E. L.; Yi, S. S.; Weisshaar, J. C. *Int. J. Mass Spectrom.* **2000**, *196*, 55. (c) Wen, Y.; Poremski, M.; Ferrett, T. A.; Weisshaar, J. C. *J. Phys. Chem. A* **1998**, *102*, 8362. (d) Carroll, J. J.; Haug, K. L.; Weisshaar, J. C. *J. Am. Chem. Soc.* **1993**, *115*, 6962. (e) Poremski, M.; Weisshaar, J. C. *J. Phys. Chem. A* **2000**, *104*, 1524. (f) Rivalta, I.; Russo, N.; Sicilia, E. *THEOCHEM* **2006**, *762*, 25.

(6) (a) Hinrichs, R. Z.; Schroden, J. J.; Davis, H. F. *J. Am. Chem. Soc.* **2003**, *125*, 860. (b) Schroden, J. J.; Wang, C. C.; Davis, H. F. *J. Phys. Chem. A* **2003**, *107*, 9295. (c) Porembski, M.; Weisshaar, J. C. *J. Phys. Chem. A* **2001**, *105*, 6655. (d) Stauffer, H. U.; Hinrichs, R. Z.; Schroden, J. J.; Davis, H. F. *J. Phys. Chem. A* **2000**, *104*, 1107. (e) Hinrichs, R. Z.; Schroden, J. J.; Davis, H. F. *J. Phys. Chem. A* **2003**, *107*, 9284. (f) Willis, P. A.; Stauffer, H. U.; Hinrichs, R. Z.; Davis, H. F. *J. Phys. Chem. A* **1999**, *103*, 3706.

(7) (a) Siegbahn, P. E. M.; Blomberg, M. R. A.; Svensson, M. *J. Am. Chem. Soc.* **1993**, *115*, 1952. (b) Blomberg, M. R. A.; Siegbahn, P. E. M.; Svensson, M. *J. Phys. Chem.* **1992**, *96*, 9794. (c) Blomberg, M. R. A.; Siegbahn, P. E. M.; Yi, S. S.; Noll, R. J.; Weisshaar, J. C. *J. Phys. Chem. A* **1999**, *103*, 7254.

(8) (a) Carroll, J. J.; Haug, K. L.; Weisshaar, J. C.; Blomberg, M. R. A.; Siegbahn, P. E. M.; Svensson, M. *J. Phys. Chem.* **1995**, *99*, 13955. (b) Carroll, J. J.; Weisshaar, J. C. *J. Phys. Chem.* **1996**, *100*, 12355.

(9) Poremski, M.; Weisshaar, J. C. *J. Phys. Chem. A* **2001**, *105*, 4851.

(10) Lee, Y. K.; Manceron, L.; Papai, I. *J. Phys. Chem. A* **1997**, *101*, 9650.

(11) (a) Cho, H.-G.; Andrews, L. *J. Phys. Chem. A* **2004**, *108*, 3965. (b) Cho, H.-G.; Andrews, L. *J. Phys. Chem. A* **2004**, *108*, 10441.

(12) Cho, H.-G.; Andrews, L. *J. Phys. Chem. A* **2007**, *111*, 5201.

(13) Cho, H.-G.; Andrews, L. *J. Phys. Chem. A* **2008**, *112*, 12071.

(14) (a) Cho, H.-G.; Lyon, J. T.; Andrews, L. *J. Phys. Chem. A* **2008**, *112*, 6902. (b) Andrews, L.; Cho, H.-G. *J. Phys. Chem. A* **2005**, *109*, 6796. (c) Andrews, L.; Kushto, G. P.; Marsden, C. J. *Chem.−Eur. J.* **2006**, *12*, 8324.

(15) (a) Andrews, L.; Citra, A. *Chem. Rev.* **2002**, *102*, 885. (b) Andrews, L. *Chem. Soc. Rev.* **2004**, *33*, 123.

(16) Frisch, M. J.; Trucks, G. W.; Schlegel, H. B.; Scuseria, G. E.; Robb, M. A.; Cheeseman, J. R.; Montgomery, J. A., Jr.; Vreven, T.; Kudin, K. N.; Burant, J. C.; Millam, J. M.; Iyengar, S. S.; Tomasi, J.; Barone, V.; Mennucci, B.; Cossi, M.; Scalmani, G.; Rega, N.; Petersson, G. A.; Nakatsuji, H.; Hada, M.; Ehara, M.; Toyota, K.; Fukuda, R.; Hasegawa, J.; Ishida, M.; Nakajima, T.; Honda, Y.; Kitao, O.; Nakai, H.; Klene, M.; Li, X.; Knox, J. E.; Hratchian, H. P.; Cross, J. B.; Bakken, V.; Adamo, C.; Jaramillo, J.; Gomperts, R.; Stratmann, R. E.; Yazyev, O.; Austin, A. J.; Cammi, R.; Pomelli, C.; Ochterski, J. W.; Ayala, P. Y.; Morokuma, K.; Voth, G. A.; Salvador, P.; Dannenberg, J. J.; Zakrzewski, V. G.; Dapprich, S.; Daniels, A. D.; Strain, M. C.; Farkas, O.; Malick, D. K.; Rabuck, A. D.; Raghavachari, K.; Foresman, J. B.; Ortiz, J. V.; Cui, Q.; Baboul, A. G.; Clifford, S.; Cioslowski, J.; Stefanov, B. B.; Liu, G.; Liashenko, A.; Piskorz, P.; Komaromi, I.; Martin, R. L.; Fox, D. J.; Keith, T.; Al-Laham, M. A.; Peng, C. Y.; Nanayakkara, A.; Challacombe, M.; Gill, P. M. W.; Johnson, B.; Chen, W.; Wong, M. W.; Gonzalez, C.; Pople, J. A. *Gaussian 03*, revision C.02; Gaussian, Inc.: Wallingford, CT, 2004.

(17) (a) Becke, A. D. *J. Chem. Phys.* **1993**, *98*, 5648. (b) Lee, C.; Yang, Y.; Parr, R. G. *Phys. Rev. B* **1988**, *37*, 785.

(18) Raghavachari, K.; Trucks, G. W. *J. Chem. Phys.* **1989**, *91*, 1062.

(19) Küchle, W.; Dolg, M.; Stoll, H.; Preuss, H. *J. Chem. Phys.* **1994**, *100*, 7535.

(20) Burke, K.; Perdew, J. P.; Wang, Y. In *Electronic Density Functional Theory: Recent Progress and New Directions*; Dobson, J. F., Vignale, G., Das, M. P., Eds.; Plenum: 1998.

(21) (a) Scott, A. P.; Radom, L. *J. Phys. Chem.* **1996**, *100*, 16502. (b) Andersson, M. P.; Uvdal, P. L. *J. Phys. Chem. A* **2005**, *109*, 2937.

(22) (a) Souter, P. F.; Kushto, G. P.; Andrews, L.; Neurock, M. *J. Phys. Chem. A* **1997**, *101*, 1287. (b) Liang, B.; Andrews, L.; Li, J.; Bursten, B. E. *J. Am. Chem. Soc.* **2002**, *124*, 6723.

(23) (a) Reed, A. E.; Weinstock, R. B.; Weinhold, F. *J. Chem. Phys.* **1985**, *83*, 735. (b) Reed, A. E.; Curtiss, L. A.; Weinhold, F. *Chem. Rev.* **1988**, *88*, 899.

(24) (a) Wang, X.; Andrews, L. *J. Phys. Chem. A* **2002**, *106*, 6720. (b) Wang, X.; Andrews, L. *J. Phys. Chem. A* **2005**, *109*, 9021. (c) Wang, X.; Andrews, L. *J. Phys. Chem. A* **2003**, *107*, 570.

(25) (a) Lyon, J. T.; Andrews, L.; Malmqvist, P.-Å.; Roos, B. O.; Yang, T.; Bursten, B. E. *Inorg. Chem.* **2007**, *46*, 4917. (b) Souter, P. F.; Kushto, G. P.; Andrews, L.; Neurock, M. *J. Am. Chem. Soc.* **1997**, *119*, 1682.

(26) Hunt, R. D.; Yustein, J. T.; Andrews, L. *J. Chem. Phys.* **1993**, *98*, 6070.

JP900610C